Bulgarian Chemical Communications, Volume 52, Special Issue E (pp. 5-14) 2020

Graphene-based poly(vinyl alcohol)/chitosan hydrogels with electrochemically synthesized silver nanoparticles for medical applications – a review

Katarina R. Nešović, Vesna B. Mišković-Stanković*

University of Belgrade, Faculty of Technology and Metallurgy, Karnegijeva 4, Belgrade, Serbia

Received January 20, 2020; Accepted February 13, 2020

Silver nanoparticles (AgNPs) have become an interesting alternative to antibiotics for potential applications in biomedicine, since nanocrystalline silver is proved to be highly efficient antimicrobial agent with a wide inhibiting spectrum against many types of microorganisms. AgNPs embedded in hydrogel matrices are attractive for biomedical applications due to the possibility for their controlled release resulting in enhanced antimicrobial activity. Thus, combination of AgNPs with biocompatible hydrogels, poly(vinyl alcohol) (PVA) and chitosan (CHI), provides potential for design of improved medical treatments and devices (antimicrobial wound dressings, soft tissue implants). Graphene (Gr) has exceptional mechanical properties and has therefore been applied as adequate reinforcing component for polymer-based composite materials. The synthesis of AgNPs is always subject to innovation and improvements, as it is desirable to minimize the use of chemical agents with the aim of improving the biocompatibility of the obtained material. With this in mind, a green alternative to traditional chemical synthesis methods would be the electrochemical reduction of silver ions, especially as this method provides the option of direct in situ synthesis of AgNPs inside the polymer matrix. In this paper, we provide an overview of the state of the art regarding graphene-reinforced polymer matrices with electrochemically synthesized silver nanoparticles for medical application. We show that the electrochemical method of AgNPs synthesis in PVA/CHI hydrogel matrices has emerged as an excellent method to obtain nanoparticles, and that the incorporation of graphene improved the hydrogels` mechanical properties and elasticity.

Keywords: graphene, chitosan, silver nanoparticles, electrochemical synthesis, hydrogel

INTRODUCTION

Recent trends in biomedical materials science have emerged regarding the research of novel wound dressing materials to improve their antibacterial and anti-inflammatory properties, as well as longevity and controlled delivery of active components. These are the most prominent features where the traditional dressing materials come short, as they have some glaring drawbacks, especially when it comes to treating chronic wounds. Particularly big problem is the need for almost daily replacement of gauzes and cotton bandages, due to their susceptibility to bacterial colonization and proneness to dry out and adhere to the newly-grown fibrous tissue on the wound [1,2]. Hydrophilic polymers represent an exciting perspective to overcome these drawbacks, as they are a group of materials with many possibilities that can be tailored to suit the needs of chronic wound patients. Hydrogels based on both synthetic and natural-origin polymers have emerged as prospective moisture-retentive wound dressing materials for long-lasting wound healing applications [1,3]. Poly(vinyl alcohol) (PVA) is a synthetic polymer with exceptional biocompatibility that has been used in bio-applications for over half a century [4], and it provides a great structural matrix for hydrogel wound dressings, due to its ability to form physically cross linked hydrogels via the facile freezing-thawing route [5]. PVA is often blended with natural-origin polymers to improve its bioactivity, such as polysaccharide chitosan (CHI), which is a partially deacetylated derivate of chitin – long-chain N-acetylglucosamine polymer derived from crustacean exoskeletons and fungi cell walls [6]. CHI, an acidic media-soluble polymer, is an exciting component for wound dressing materials, due to its intrinsic antibacterial activity that stems from the presence of protonated $–NH_3^+$ groups on its chain [7], as well as due to the well-documented ability to provide an excellent matrix for immobilization of antibacterial metallic nanoparticles [8,9]. Out of the many metals used in antibacterial applications, silver nanoparticles (AgNPs) have long been known as one of the strongest and most versatile antimicrobial agents with a broad-spectrum activity against many microorganisms [10,11]. The nanocrystalline form of silver has been shown to possess enhanced antibacterial activity compared to silver-ion

* To whom all correspondence should be sent.
E-mail: vesna@tmf.bg.ac.rs

formulations, due to the multi-faceted mode of action as well as the ability to also release Ag^+ ions through oxidative dissolution in aqueous physiological media [10]. AgNPs also exhibit size-dependent activity – the smaller the nanoparticle, the higher the antibacterial effect [12]. High surface energy of very small AgNPs makes them very unstable though, so they are usually stabilized inside polymer matrices, such as hydrogels, to ensure long-term efficiency [12]. Of the many methods to synthesize AgNPs in a hydrogel matrix, *in situ* electrochemical route has emerged as a facile and green alternative to the usual chemical reduction [13–15]. The obtained AgNP-loaded hydrogels can, however, suffer from poor mechanical properties and susceptibility to degradation, especially chitosan-based blends, due to the poor mechanical strength of CHI [16]. Thus, research has shown that hydrogels can be reinforced by the means of a nano-filler addition, such as graphene (Gr), which can improve the stability of the hydrogel even at small loading amounts [17–20]. Gr, the two-dimensional (2D) prodigy of a material, has many exceptional properties [21], and has found a versatile application even in biomedical materials fields [22].

In this work, we provide a brief overview of PVA and chitosan-based, graphene-reinforced hydrogel materials with antibacterial electrochemically-synthesized AgNPs for next-generation wound dressing materials.

Graphene-based hydrogels for medical applications.

Since its discovery at the beginning of this century, graphene (Gr) has revolutionized many areas of materials science and opened up a plethora of new possibilities and research directions. A honeycomb 2D lattice of carbon atom monolayer, graphene has exhibited many fantastic expected and unexpected properties [21], which opened the door to its applications in broadest spectrum of materials science and engineering fields. Graphene has shown such diverse applicability which one would not think possible and it is researched for applications in electronics [23], photovoltaics [24], energy storage [25,26], biosensors [27]. Aside from its special properties such as mechanical strength, electrical conductivity, zero-bandgap semiconductivity [21] and high specific surface area [22], Gr was even shown to exhibit antibacterial activity that gave rise to significant interest in graphene nanocomposites bio-applications such as wound dressings or drug delivery [22].

Composite polymer hydrogels with added graphene or its derivatives such as graphene oxide (GO), have drawn significant attention in wound dressing and tissue engineering fields [22]. Fan et al. [28] have shown that konjac glucomannan/carboxymethyl chitosan/graphene oxide wound dressings exhibited significant increase in compressive strength and modulus, as well as improved biocompatibility towards NIH-3T3 mouse embryonic cells with increased GO content; whereas it was also shown that GO incorporation improved Young's modulus, maximum compression stress and strain of poly (acrylic acid)/gelatin hydrogels [29]. Gelatin methacrylate hydrogels with incorporated GO also enhanced proliferation of HaCaT keratinocyte cells [30]. An interesting study showed that free-standing graphene hydrogels could possess osteoinductivity and ability to promote bone tissue regeneration, as confirmed by both *in vitro* and *in vivo* tests [31]. Sodium carboxymethyl cellulose/reduced graphene oxide hydrogels exhibited anti-biofilm activity, reducing *S. aureus* and *P. aeruginosa* biofilm formation by ~80% and ~60%, respectively [32]. Ag/graphene composite hydrogels cross linked with acrylic acid and N,N′-methylenebis(acrylamide) possessed strong *in vitro* antibacterial activity and enhanced *in vivo* wound healing [33]. Ma et al. [34] showed that sodium alginate/graphene oxide (GO)/poly(vinyl alcohol) nanocomposite sponges loaded with norfloxacin had excellent antibacterial activity against *E. coli* and *S. aureus*, while also promoting wound healing *in vivo*. Another study investigated ciprofloxacin-loaded chitosan/poly(vinyl alcohol)/graphene oxide nanofibrous membranes and confirmed significant inhibitory effect against *E. coli*, *S. aureus* and *B. subtilis*, along with good cytocompatibility [35]. Bacterial nanocellulose/poly(acrylic acid)/graphene oxide composite hydrogels promoted attachment and proliferation of human dermal fibroblast cells, indicating good wound healing potential [36]. Graphene was also incorporated in poly(vinyl alcohol) [14,18,37–39] and poly(vinyl alcohol)/chitosan [13,15,17,40,41] hydrogels and films with incorporated silver nanoparticles (AgNPs) for wound dressing applications, where it was shown that very small amounts of Gr improved elasticity and strength of these wound dressing materials [17,18].

Quite obviously, graphene has found wide application in biomedical field, and this short review will cover some aspects of graphene-loaded hydrogels based on poly(vinyl alcohol) and chitosan polymers, as antibacterial wound dressing materials.

Silver nanoparticles as an antibacterial agent and their electrochemical synthesis.

Silver nanoparticles have long been recognized and established as one of the strongest antimicrobial agents [11], with broad-spectrum performance and without the inherent risks associated with antibiotics that are well known to quickly induce bacterial resistance, due to their targeted modes of action [42]. The modes of action of AgNPs have been long and widely investigated, and covered in several comprehensive reviews [11,12,43]. Most studies agree that the AgNPs antibacterial activity stems from their large surface area that allows direct contact with the bacterial cell wall, which results in various types of membrane damage, cytoplasm leakage as well as in penetration inside the cell itself [12,43]. Further, the AgNPs can participate in generation of reactive oxygen species (ROS), as well as undergo oxidative dissolution, resulting in the release of Ag^+ ions, which, in turn, also possess significant antibacterial activity [44]. The antibacterial activity of AgNPs is also known to be dose-dependent and size-dependent, with most research works indicating that the nanoparticles smaller than 10 nm, exhibit the strongest antibacterial effect [12]. As described above, the mode of action is very versatile, which makes it difficult for bacteria to develop resistance mechanism, rendering the AgNPs an excellent choice for an active agent in wound dressings for long-term application. However, a non-negligible risk with silver nanoparticles application is their documented toxicity towards healthy mammalian cells [12]. The mechanisms of AgNP cytotoxicity are similar to those of their antibacterial action, with cellular uptake, Ag^+ release, DNA and protein damage, and ROS generation being some of the most widely cited causes of toxicity [12]. Besides dose-dependent cytotoxicity, a major issue is also potential accumulated toxicity caused by accumulation of smaller amounts of silver in cells and tissue over longer periods of time [12,45]. Therefore, when designing silver-containing wound dressing material, the dose is of crucial importance and the release effects must be taken into account, in order to achieve a product which can retain antibacterial properties for long time periods, all the while not posing a threat towards the healthy tissue.

One of the most reliable methods to obtain silver nanoparticles in polymer gels and dispersions is certainly electrochemical synthesis [14,15,37, 40,46]. The merits of this method include one-step setup and the avoidance of possibly toxic chemical agents for Ag^+ reduction. There are various electrochemical techniques for AgNPs synthesis, including reduction in polymer dispersion, where the AgNPs are stabilized by polymer chains [37,46,47], as well as *in situ* reduction in a hydrogel matrix, where the main purpose of electric current is to serve as an intermediary to produce hydrogen gas on the cathode, which then permeates the hydrogel, reacting with Ag^+ ions to form nucleation sites for the formation of AgNPs [13,17]. One such principal scheme for this type of *in situ* electrochemical synthesis is presented in Fig. 1, showing that the hydrogel, pre-swollen in Ag^+ precursor solution (usually $AgNO_3$ of desired concentration) is placed between the two platinum plates that serve as working and counter electrodes, and are connected to a DC power source, used to supply a constant voltage. Briefly, the hydrogels were obtained by first preparing the PVA/chitosan/graphene colloid dispersions without CHI and with 0.1 wt% CHI (PVA/0.1CHI/Gr) and 0.5 wt% CHI (PVA/0.5CHI/Gr), pouring them into Petri dishes up to 5 mm height and then cross linking by the physical freezing-thawing technique [15,17,40]. After 5 cycles of freezing and thawing, the hydrogels were cut to 10 mm × 5 mm discs and the electrochemical synthesis was performed as follows. The obtained hydrogel discs were immersed in 3.9 mM $AgNO_3$ precursor swelling solution and swollen for 48 h, after which they were placed in the electrochemical cell depicted in Fig. 1 and subjected to 90 V constant DC voltage, to obtain silver-loaded hydrogels (3.9Ag/PVA/Gr, 3.9Ag/PVA/0.1CHI/Gr and 3.9Ag/PVA/0.5CHI/Gr) [15,17,40].

The advantage of this *in situ* method is the fact that the synthesis is performed in a single step, and the final product is a nanocomposite hydrogel with incorporated AgNPs, which is completely biocompatible and there is no need to perform subsequent washing and extraction of unreacted chemicals, as is the case with the chemical AgNP synthesis method. A representative photograph of poly(vinyl alcohol)/chitosan/graphene (PVA/ CHI/Gr) and silver/poly(vinyl alcohol)/chitosan/ graphene (Ag/PVA/CHI/Gr) hydrogels, obtained using the above-described method is shown in Fig. 2 – typical yellow coloration of the hydrogel sample in Fig. 2b attests to the successful formation of AgNPs.

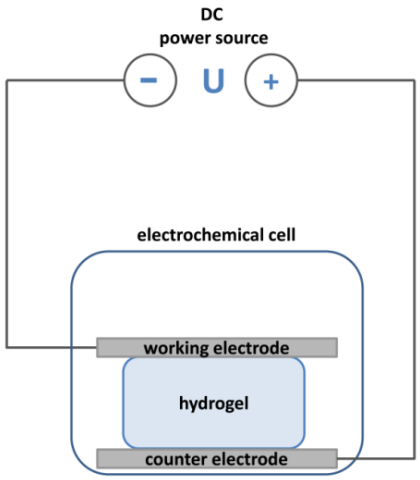

Fig. 1. Scheme of the electrochemical setup for the synthesis of silver/poly(vinyl alcohol)/chitosan/graphene hydrogel

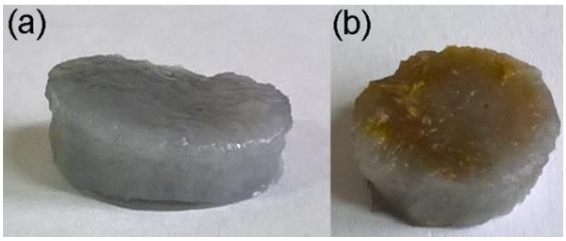

Fig. 2. Images of (a) poly(vinyl alcohol)/chitosan/graphene and (b) silver/poly(vinyl alcohol)/chitosan/graphene hydrogels

Chitosan has been repeatedly shown to significantly influence the formation and concentration of AgNPs inside the hydrogel matrices, as confirmed by much higher absorbance value in the UV-vis spectrum of hydrogel containing CHI, compared to that without it (Fig. 3) [15, 17]. A plausible explanation would be the mild reducing properties of CHI itself that could contribute to the quicker formation of AgNPs inside the CHI-containing hydrogels. This effect will be examined in a bit more detail in the following sections.

The effect of graphene on the properties of PVA/CHI hydrogels with AgNPs.

Mechanical strength and elasticity are some of the most important physical properties of a wound dressing, which can ensure prolonged structural integrity of the dressing material that is usually to be used over longer time periods. Graphene, when used as a nano-filler inside three-dimensional (3D) polymer matrices, is known to dramatically improve their mechanical properties, such as elasticity or yield strength [20,29].

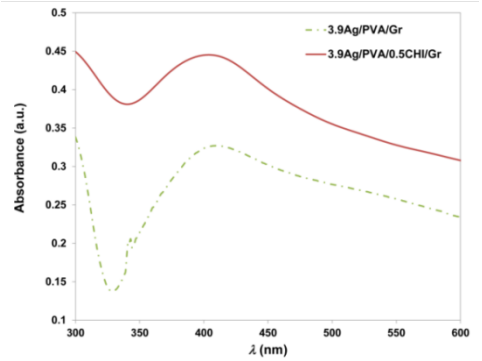

Fig. 3. Representative UV-vis spectra of silver/poly(vinyl alcohol)/graphene hydrogels (3.9Ag/PVA/Gr) and silver/poly(vinyl alcohol)/0.5 wt% chitosan/graphene hydrogels (3.9Ag/PVA/0.5CHI/Gr) hydrogels, showing characteristic absorbance maximum of AgNPs at ~400 nm.

Loading small amounts of Gr in polymeric matrices has been shown to improve mechanical properties of poly (acrylic acid) [48], polylactide/poly(ε-caprolactone) blend [49], as well as poly(vinyl alcohol) [18,50] and poly(vinyl alcohol)/chitosan hydrogels [17]. For example, the effect of graphene loading on the mechanical properties and elasticity of poly(vinyl alcohol)/chitosan matrices, can be seen very distinctively from the Table 1 [17]. Films with 10 wt% PVA and varying amounts of chitosan – 0.1 wt% (PVA/0.1CHI) and 0.5 wt% (PVA/0.5CHI) were prepared, and it was observed (as expected) that the increased amount of chitosan decreased the overall mechanical stability of PVA/0.5CHI, which exhibited much lower yield strength as well as elasticity modulus [17]. On the other hand, the addition of very small amount of graphene (0.01 wt%) drastically increased both elasticity modulus and yield and ultimate strength of the PVA/0.5CHI/Gr sample (Table 1) [17]. Other studies have confirmed the same, showing that Gr can be used as a very strong reinforcing material which imparts excellent mechanical strength and elastic properties upon hydrogel matrices – which is especially important when using such natural-origin biopolymers with poor intrinsic mechanical properties, as chitosan.

Table 1. Mechanical properties of PVA/0.1CHI, PVA/0.5CHI and PVA/0.5CHI/Gr: σ_R – tensile yield strength, ε_R – yield elongation, E_J – Young's elasticity modulus, σ_U – ultimate strength, ε_U – ultimate elongation. Reprinted from [17] with permission from Elsevier (Copyright 2019).

	σ_R (MPa)	ε_R (%)	E_J (MPa)	σ_U (MPa)	ε_U (%)
PVA/0.1CHI	30.7	2.7	21.4	38.5	28.1
PVA/0.5CHI	22.6	3.8	14.0	24.4	38.0
PVA/0.5CHI/Gr	78.0	1.3	121.7	63.1	23.2

However, graphene could not only influence mechanical properties of wound dressing nanocomposite materials. Gr has also been shown to affect the formation and stabilization of AgNPs inside the polymer matrix [51,52], although these effects have not been investigated thoroughly. UV-vis spectroscopy is a fairly reliable method to assess the amounts/concentrations of incorporated silver nanoparticles, as they give rise to quite distinctive peaks in the lower visible region, known as surface plasmon resosnance (SPR) maxima [53]. When comparing the obtained UV-vis spectra for hydrogels with different amounts of chitosan (0, 0.1 and 0.5 wt%) [15,17,40], the first thing to be noticed is that hydrogels with higher chitosan content (Ag/PVA/0.5CHI/Gr) exhibited higher maximum absorbance (A_{max}=1.6), compared to both Ag/PVA/Gr (A_{max}=0.45) and Ag/PVA/0.1CHI/Gr (A_{max}=1.05) [15] pointing to higher amount of AgNPs due to additional reduction on CHI chains, as already briefly discussed above. Further, it can be noticed that hydrogels containing graphene also possessed higher absorbance of their SPR peak, and therefore higher AgNP concentration, compared to their counterparts without Gr [13,15,17,40]. For example, 3.9Ag/PVA/0.1CHI/Gr (A_{max}=1.05 [15]) and 3.9Ag/PVA/0.5CHI/Gr (A_{max}=1.6 [15]) hydrogels exhibited higher A_{max} than 3.9Ag/PVA/0.1CHI (A_{max}=0.3 [13]) and 3.9Ag/PVA/0.5CHI (A_{max}=1.0 [13]), respectively, which is also true for 0.25Ag/PVA/0.1CHI/Gr (A_{max}=0.1 [40]) and 0.25Ag/PVA/0.5CHI/Gr (A_{max}=0.41 [40]) hydrogels, compared to 0.25Ag/PVA/0.1CHI (A_{max}=0.05 [13]) and 0.25Ag/PVA/0.5CHI (A_{max}=0.17 [13]), respectively. Obviously, graphene can affect the formation and stabilization of AgNPs inside polymer matrices, likely through interactions and shielding nanoparticles from agglomeration, as it was shown before that Gr and Gr oxide can be even used as effective dispersion agents to support metal nanoparticles [52,54,55].

A complementary dynamic light scattering (DLS) technique revealed average hydrodynamic diameters of the obtained nanoparticles to be 8.06 ± 0.098 nm for Ag/PVA/0.1CHI/Gr and 6.38 ± 0.12 nm for Ag/PVA/0.5CHI/Gr [17], indicating a strong influence of increased chitosan content on stabilization and consequent smaller size of AgNPs in the hydrogel.

These findings indicate that CHI plays a significant role in nanoparticle stabilization, which was also confirmed by transmission electron microscopy (TEM) (Fig. 4) [13,17]. TEM analysis indicated the incorporation of even very small nanoparticles inside the hydrogel matrices, such as the nanoparticle in Fig. 4d, sized around 2-3 nm in 3.9Ag/PVA/0.5CHI/Gr hydrogel. The statistical distribution of AgNPs obtained by DLS, coupled with the microscopic TEM investigation, confirmed the incorporation of very small AgNPs (<10 nm) inside hydrogels both with and without graphene, pointing to their strong potential as antibacterial agents for wound dressing.

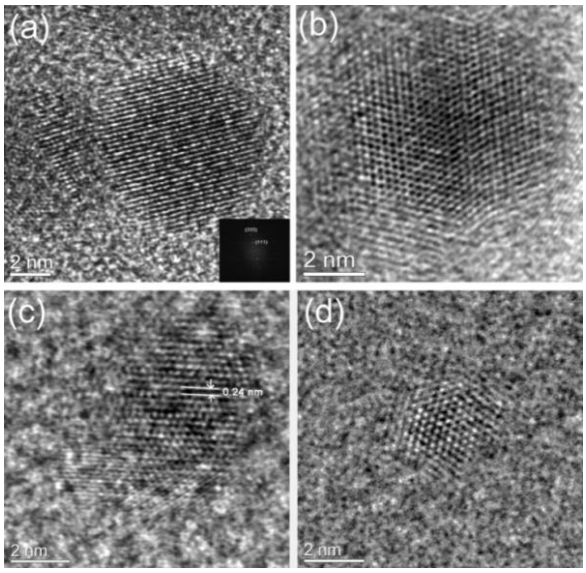

Fig. 4. TEM micrographs of (a) 3.9Ag/PVA/0.1CHI, (b) 3.9Ag/PVA/0.5CHI, (Reprinted from [13] with permission from Elsevier (Copyright 2019)) (c) 3.9Ag/PVA/0.1CHI/Gr and (d) 3.9Ag/PVA/0.5CHI/Gr (Reprinted from [17] with permission from Elsevier (Copyright 2019)).

Application of graphene-based poly(vinyl alcohol)/chitosan hydrogels with AgNPs – silver release and antibacterial properties.

As already mentioned, when designing a new wound dressing material with an active antibacterial component, it is very important to determine the release behavior of this agent, in order to tailor the properties of the dressing to achieve the optimal infection protection. The release measurements are usually carried out at 37°C, in some physiological buffer, such as phosphate buffer (PB) that mimics the physiological environment in human organism. In addition, the non-toxicity requirements for wound dressings dictate the incorporation of smaller amounts of AgNPs in order to achieve the best antibacterial effect without inducing any cytotoxic response [13,17]. Thus, for *in vitro* silver release and antibacterial experiments, hydrogels were prepared from lower-concentration precursor swelling solution (0.25 mM $AgNO_3$) [13,17,40]. Fig. 5 shows representative silver release profiles for 0.25Ag/PVA/0.1CHI/Gr and 0.25Ag/PVA/0.5CHI/Gr hydrogels, which were measured over 28-day period [40]. The release curves provide several interesting observations, the first being that the total initial concentration of AgNPs was higher in 0.25Ag/PVA/0.5CHI/Gr hydrogel (80 mg dm^{-3}), compared to 0.25Ag/PVA/0.1CHI/Gr (55 mg dm^{-3}) [40]. Further, the release profiles exhibited typical burst release in initial 3-5 days, followed by slower period until finally reaching a plateau. The 0.25Ag/PVA/0.5CHI/Gr hydrogel also retained higher amount of silver after 28 days (~50 mg dm^{-3}), in comparison with 0.25Ag/PVA/0.1CHI/Gr (~30 mg dm^{-3}), ensuring that the hydrogel maintained sterility over prolonged time period.

More information from the release profiles can be extracted by fitting with well-known theoretical models that could be used to elucidate the kinetics of silver release. Some of the most common models – zero, first and second order kinetics – are presented in Table 2, along with equations that describe them and rate constant parameters that can be calculated from the fit. The silver release profiles, fitted with models from Table 2, for 0.25Ag/PVA/0.1CHI/Gr and 0.25Ag/PVA/0.5CHI/Gr hydrogels are shown in Fig. 6.

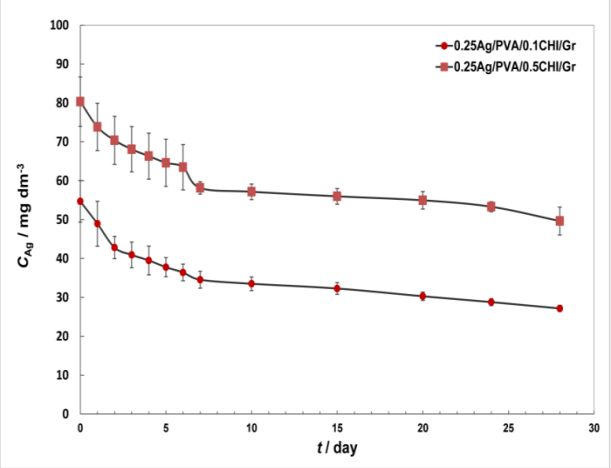

Fig. 5. Silver release profiles for 0.25Ag/PVA/0.1CHI/Gr and 0.25Ag/PVA/0.5CHI/Gr hydrogels [40]

Table 2. Kinetic models used to fit silver release profiles [41].

Model name	Equation	Constants
Zero order	$c_{Ag} = c_{Ag,0} - k_0 \cdot t$	k_0 – zero-order rate constant
First order	$\ln c_{Ag} = \ln c_{Ag,0} - k_1 \cdot t$	k_1 – first-order rate constant
Second order	$\frac{1}{c_{Ag}} = \frac{1}{c_{Ag,0}} + k_2 \cdot t$	k_2 – second-order rate constant

From Fig. 6, it can be observed that the release profiles cannot be fitted with one model over the entire release period, rather they are split into three, and two stages for 0.25Ag/PVA/0.1CHI/Gr and 0.25Ag/PVA/0.5CHI/Gr, respectively. The first stage that corresponds to shorter release times is characteristic for burst release behavior, where the release is quicker upon initial immersion of the hydrogel in PB medium. This first period is described by higher values of rate constants for all three models (Fig. 6), compared to the latter period that corresponds to the time needed to reach the plateau on the release profile. In the case of 0.25Ag/PVA/0.1CHI/Gr, the burst release period actually comprised two stages with different release rates, indicating that the fastest release of AgNPs is actually achieved between 2 and 7 days. This delay in silver release in the first 48 h might not be ideal for wound dressing applications, as it is crucially important to achieve the highest initial inflow of the

antibacterial agent to the wound area, especially in this initial 2-day period. Therefore, the hydrogel with higher chitosan content (0.25Ag/PVA/0.5CHI/Gr) might be a better option for wound dressing material, as it does not show this discrepancy, exhibiting instead a smooth burst release period lasting up to 7 days. In addition, 7 days is a fairly long period for fast release, so these hydrogels would also possess a very desirable property of retaining antibacterial activity and maintaining long-lasting wound sterility, without the need for frequent replacements [40].

It should be also noted that all three kinetic models provided satisfactory correlation with the experimental data, especially for 0.25Ag/PVA/0.1CHI/Gr hydrogel, and especially in the initial burst release period. However, the best model should be chosen by evaluation of parameters in all stages, and it was found that the second order model provided the best fit for both hydrogel samples and for all release periods (R^2>0.99 for burst period, and R^2>0.97 for long-term release). Another interesting observation could be made by comparing the results presented here with the release models for hydrogels without graphene from our previous study (0.25Ag/PVA/0.1CHI and 0.25Ag/PVA/0.5CHI) [41]. Hydrogels without graphene were also found to exhibit second-order kinetics of silver release [41]; however, for those samples only one smooth period was observed upon fitting with the second-order model. Obviously, the Gr-containing hydrogels exhibited different behavior, releasing silver in several stages with different rates, as shown in Fig. 6 and discussed above. These findings indicate that Gr could play a role in AgNPs stabilization, and that the interactions between Gr sheets and AgNPs might account for different release behavior of these hydrogels in comparison with their counterparts without Gr.

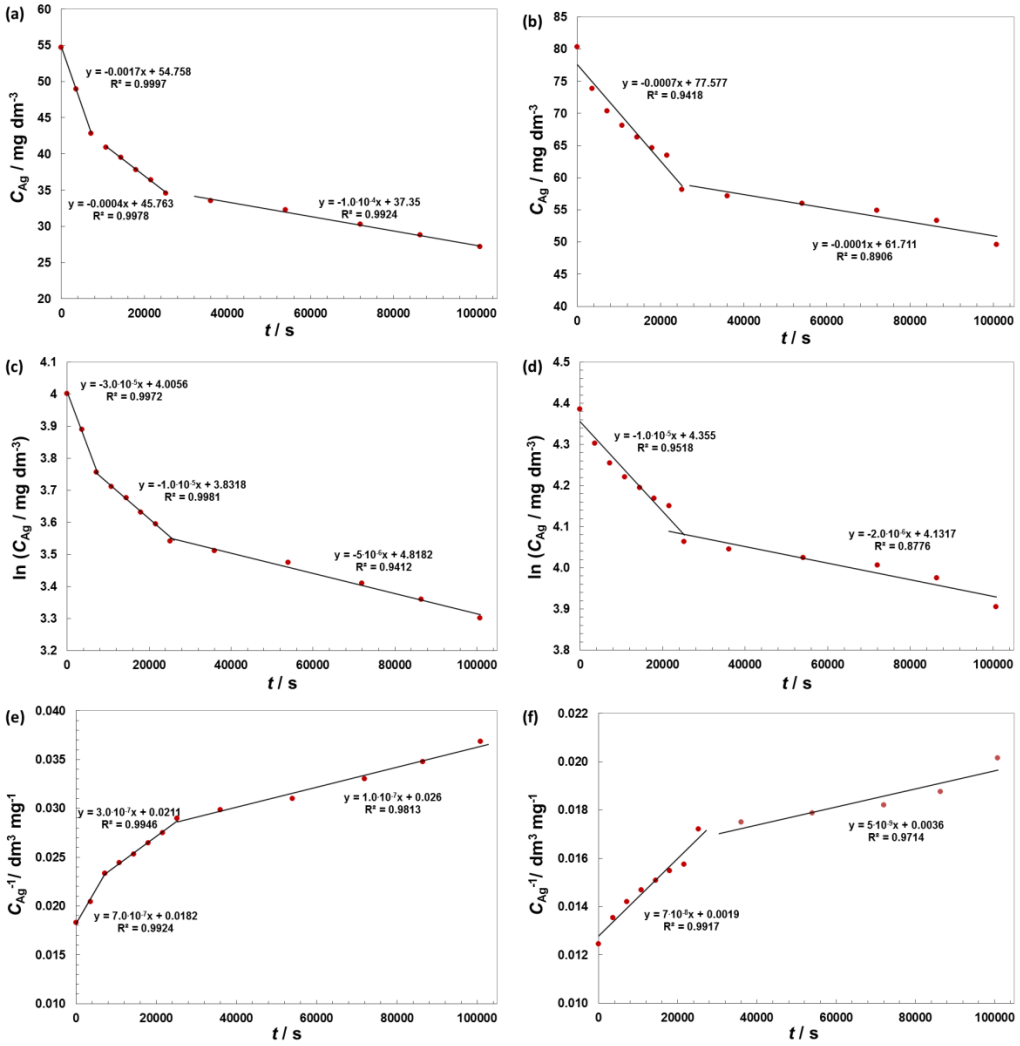

Fig. 6. Different models of silver release for (a,c,e) 0.25Ag/PVA/0.1CHI/Gr and (b,d,f) 0.25Ag/PVA/0.5CHI/Gr hydrogels: (a,b) zero, (c,d) first and (e,f) second order kinetics.

Finally, one of the most important properties of next-generation wound dressing materials is certainly their antibacterial activity. The requirements for a wound dressing are usually such that it needs to provide a long lasting antibacterial effect and sustained release of the active component to the wound area, in order to efficiently combat the colonization of bacteria. Especially critical are the first 24-48 h, when bacteria usually begin to form a biofilm and therefore it is imperative to achieve the most efficient antibacterial action in this period. This effect can also be accomplished by synergistic action of several antibacterial components, as is the case with chitosan-containing hydrogels with AgNPs [13,17,40,56]. Chitosan is a known intrinsically bactericidal polymer [7,57], whereas AgNPs act as a main agent that is to be released gradually for long-term protection of the wound. Furthermore, graphene has also been shown to be a potential antibacterial agent in certain cases [22,28,34,58]. One of the main culprits for wound infections is *Staphylococcus aureus* species [59], which normally inhabits the human skin, but can wreak havoc if it infects a wound. Another bacterial strain often found in wound infections is the Gram-negative *Escherichia coli*. Table 3 shows the results of quantitative antibacterial suspension tests against *S. aureus* and *E. coli* for 0.25Ag/PVA/0.1CHI/Gr and 0.25Ag/PVA/0.5CHI/Gr hydrogels [17]. It can be observed that both hydrogels exhibited significant antibacterial activity after only 15 min, causing significant reduction in CFU counts of around 1 logarithmic unit. Furthermore, the hydrogel with higher CHI content (0.25Ag/PVA/0.5CHI/Gr), caused faster inhibition of bacterial viability after 15 min, compared to 0.25Ag/PVA/0.1CHI/Gr, pointing to strong influence of CHI on the hydrogel bactericidal action. After 15 min, there were $0.021x10^5$ CFU ml^{-1} *S. aureus* cells remaining in the presence of 0.25Ag/PVA/0.5CHI/Gr, compared to $0.26\ x10^5$ CFU ml^{-1} for 0.25Ag/PVA/0.1CHI/Gr [17]. In addition, 0.25Ag/PVA/0.5CHI/Gr destroyed *E. coli* cells more effectively ($1.12x10^5$ CFU ml^{-1}), compared to 0.25Ag/PVA/0.1CHI/Gr ($6.03x10^5$ CFU ml^{-1}) [17]. Thus, highly effective protection against bacteria was accomplished by chitosan-containing hydrogels, with both samples causing 100% destruction of bacterial cells after only 1 h, indicating significant synergy between CHI and AgNPs antibacterial action [13,17].

Table 3. Antibacterial test in suspension for 0.25Ag/PVA/0.1CHI/Gr and 0.25Ag/PVA/0.5CHI/Gr hydrogels with silver nanoparticles against *Staphylococcus aureus* and *Escherichia coli* – bacterial survival rates expressed as the number of colony forming units per milliliter (CFU ml^{-1}) [17]

	Number of bacterial cells (10^5 CFU ml^{-1})		
	S. aureus		
	0 h	**15 min**	**1 h**
0.25Ag/PVA/0.1CHI/Gr	0.95	0.26	0
0.25Ag/PVA/0.5CHI/Gr	0.95	0.021	0
	E. coli		
	0 h	**15 min**	**1 h**
0.25Ag/PVA/0.1CHI/Gr	16.6	6.03	0
0.25Ag/PVA/0.5CHI/Gr	16.6	1.12	0

CONCLUSIONS AND OUTLOOK

In this review, we have covered the existing research regarding poly(vinyl alcohol)/chitosan hydrogel wound dressings, reinforced by graphene filler and with silver nanoparticles, incorporated via *in situ* electrochemical synthesis method. Graphene, as a versatile material with many interesting properties has been shown to significantly improve mechanical properties of PVA and PVA/CHI hydrogels, and has even shown an indication of improved AgNPs stability in graphene-containing hydrogels. The electrochemical synthesis route is a very promising and green method to obtain silver nanoparticles directly inside the polymer matrix of a hydrogel. The AgNPs obtained by electrochemical route were shown to exhibit very small sizes (in the 2-10 nm range) and their concentration inside the hydrogel matrix can be tailored to suit the requirements of the wound dressings. Chitosan was also shown to exert a great influence on the synthesis yield, as well as on the stability and antibacterial activity of AgNPs. Hydrogels containing chitosan were shown to exhibit burst release of silver during a longer period of 7 days, which would ensure the longevity of the dressing. Furthermore, the hydrogels with CHI and AgNPs have displayed enhanced antibacterial

efficiency and bactericidal action against *S. aureus* and *E. coli* after only 1 h incubation, indicating strong synergistic effect of the polymer and the metallic component.

In perspective, hydrogel wound dressings generally are excellent alternatives for chronic wound treatments, and especially those based on PVA or chitosan. These materials have displayed exceptional tailorability of their mechanical, physico-chemical and biological properties that can be controlled by the addition of inorganic fillers such as graphene and silver nanoparticles. Importantly, hydrogels have exhibited the possibility for controlled and sustained release of the active antibacterial component, which could provide the necessary long-term infection protection to the wound area and suppress the dangerous biofilm formation. All in all, these materials show very attractive potential for wound dressing applications and next stage in research should be *in vivo* feasibility studies to confirm improvements in wound healing.

Acknowledgements: *The authors thank the Ministry of Education, Science and Technological Development of the Republic of Serbia for funding.*

REFERENCES

1. K. C. Broussard, J. G. Powers, *Am. J. Clin. Dermatol.*, **14**, 449 (2013).
2. J. S. Boateng, K. H. Matthews, H. N. E. Stevens, G. M. Eccleston, *J. Pharm. Sci.*, **97**, 2892 (2008).
3. J. G. Powers, L. M. Morton, T. J. Phillips, *Dermatol. Ther.*, **26**, 197 (2013).
4. E. A. Kamoun, E. R. S. Kenawy, X. Chen, *J. Adv. Res.*, **8**, 217 (2017).
5. S. R. Stauffer, N. A. Peppas, *Polymer.*, **33**, 3932 (1992).
6. F. Croisier, C. Jerome, *Eur. Polym. J.*, **49**, 780 (2013).
7. E. I. Rabea, M. E.-T. Badawy, C. V. Stevens, G. Smagghe, W. Steurbaut, *Biomacromolecules*, **4**, 1457 (2003).
8. S. Agnihotri, S. Mukherji, S. Mukherji, *Appl. Nanosci.*, **2**, 179 (2012).
9. Y. Murali Mohan, K. Lee, T. Premkumar, K. E. Geckeler, *Polymer*, **48**, 158 (2007).
10. D. Simões, S. P. Miguel, M. P. Ribeiro, P. Coutinho, A. G. Mendonça, I. J. Correia, *Eur. J. Pharm. Biopharm.*, **127**, 130 (2018).
11. N. Duran, M. Duran, M. B. de Jesus, A. B. Seabra, W. J. Favaro, G. Nakazato, *Nanomedicine Nanotechnology, Biol. Med.*, **12**, 789 (2016).
12. C. Liao, Y. Li, S. C. Tjong, *Int. J. Mol. Sci.*, **20**, 1 (2019).
13. K. Nešović, A. Janković, T. Radetić, M. Vukašinović-Sekulić, V. Kojić, L. Živković, A. Perić-Grujić, K. Y. Rhee, V. Mišković-Stanković, *Eur. Polym. J.*, **121**, 109257 (2019).
14. M. M. Abudabbus, I. Jevremović, K. Nešović, A. Perić-Grujić, K. Y. Rhee, V. Mišković-Stanković, *Compos. Part B Eng.*, **140**, 99 (2018).
15. K. Nešović, V. Kojić, K. Y. K. Y. Rhee, V. Mišković-Stanković, *Corrosion*, **73**, 1437 (2017).
16. S. F. Wang, L. Shen, W. De Zhang, Y. J. Tong, *Biomacromolecules*, **6**, 3067 (2005).
17. K. Nešović, A. Janković, A. Perić-Grujić, M. Vukašinović-Sekulić, T. Radetić, L. Živković, S. J. Park, K. Yop Rhee, V. Mišković-Stanković, *J. Ind. Eng. Chem.*, **77**, 83 (2019).
18. R. Surudžić, A. Janković, M. Mitrić, I. Matić, Z. D. Juranić, L. Živković, V. Mišković-Stanković, K. Y. Rhee, S. J. Park, D. Hui, *J. Ind. Eng. Chem.*, **34**, 250 (2016).
19. J. Guo, L. Ren, R. Wang, C. Zhang, Y. Yang, T. Liu, *Compos. Part B Eng.*, **42**, 2130 (2011).
20. J. H. Lee, J. Marroquin, K. Y. Rhee, S. J. Park, D. Hui, *Compos. Part B Eng.*, **45**, 682 (2013).
21. K. Geim, K. S. Novoselov, *Nat. Mater.*, **6**, 183 (2007).
22. H. Ji, H. Sun, X. Qu, *Adv. Drug Deliv. Rev.*, **105**, 176 (2016).
23. P. Avouris, *Nano Lett.*, **10**, 4285 (2010).
24. S. K. Behura, C. Wang, Y. Wen, V. Berry, *Nat. Photonics*, **13**, 312 (2019).
25. Y. Zhang, Y. An, L. Wu, H. Chen, Z. Li, H. Dou, V. Murugadoss, J. Fan, X. Zhang, X. Mai, Z. Guo, *J. Mater. Chem. A*, **7**, 19668 (2019).
26. C. Aphirakaramwong, N. Phattharasupakun, P. Suktha, A. Krittayavathananon, M. Sawangphruk, *J. Electrochem. Soc.*, **166**, A532 (2019).
27. S. K. Krishnan, E. Singh, P. Singh, M. Meyyappan, H. S. Nalwa, *RSC Adv.*, **9**, 8778 (2019).
28. L. Fan, J. Yi, J. Tong, X. Zhou, H. Ge, S. Zou, H. Wen, M. Nie, *Int. J. Biol. Macromol.*, **91**, 358 (2016).
29. S. Faghihi, M. Gheysour, A. Karimi, R. Salarian, *J. Appl. Phys.*, **115**, 083513 (2014).
30. S. R. ur Rehman, R. Augustine, A. A. Zahid, R. Ahmed, A. Hasan, *2019 41st Annu. Int. Conf. IEEE Eng. Med. Biol. Soc.*, 3943 (2019).
31. J. Lu, Y. S. He, C. Cheng, Y. Wang, L. Qiu, D. Li, D. Zou, *Adv. Funct. Mater.*, **23**, 3494 (2013).
32. N. H. Ali, M. C. I. M. Amin, S. F. Ng, *J. Biomater. Sci. Polym. Ed.*, **30**, 629 (2019).
33. Z. Fan, B. Liu, J. Wang, S. Zhang, Q. Lin, P. Gong, L. Ma, S. Yang, *Adv. Funct. Mater.*, **24**, 3933 (2014).
34. R. Ma, Y. Wang, H. Qi, C. Shi, G. Wei, L. Xiao, Z. Huang, S. Liu, H. Yu, C. Teng, H. Liu, V. Murugadoss, J. Zhang, Y. Wang, Z. Guo, *Compos. Part B Eng.*, **167**, 396 (2019).
35. S. Yang, X. Zhang, D. Zhang, *Int. J. Mol. Sci.*, **20**, 4395 (2019).
36. X. Y. Chen, H. R. Low, X. Y. Loi, L. Merel, M. A. Mohd Cairul Iqbal, *J. Biomed. Mater. Res. - Part B Appl. Biomater.*, **107**, 2140 (2019).
37. R. Surudžić, A. Janković, N. Bibić, M. Vukašinović-Sekulić, A. Perić-Grujić, V. Mišković-Stanković, S. J. Park, K. Y. Rhee, *Compos. Part B Eng.*, **85**, 102 (2016).
38. M. M. Abudabbus, I. Jevremović, A. Janković, A.

Perić-Grujić, I. Matić, M. Vukašinović-Sekulić, D. Hui, K. Y. Rhee, V. Mišković-Stanković, *Compos. Part B Eng.*, **104**, 26 (2016).
39. K. Nešović, M. M. Abudabbus, K. Y. Rhee, V. Mišković-Stanković, *Croat. Chem. Acta*, **90**, 207 (2017).
40. K. Nešović, A. Janković, V. Kojić, M. Vukašinović-Sekulić, A. Perić-Grujić, K. Y. Rhee, V. Mišković-Stanković, *Compos. Part B Eng.*, **154**, 175 (2018).
41. K. Nešović, A. Janković, T. Radetić, A. Perić-Grujić, M. Vukašinović-Sekulić, V. Kojić, K. Y. Rhee, V. Miskovic-Stankovic, *J. Electrochem. Sci. Eng.*, **10 (2)** 185 (2019).
42. G. Kapoor, S. Saigal, A. Elongavan, *J. Anaesthesiol. Clin. Pharmacol.*, **33**, 300 (2017).
43. S. Prabhu, E. K. Poulose, *Int. Nano Lett.*, **2**, 32 (2012).
44. J. R. Morones, J. L. Elechiguerra, A. Camacho, K. Holt, J. B. Kouri, J. T. Ram, M. J. Yacaman, *Nanotech*, **16**, 2346 (2005).
45. E. M. Luther, Y. Koehler, J. Diendorf, M. Epple, R. Dringen, *Nanotechnology*, **22**, 375101 (2011).
46. J. Stojkovska, D. Kostić, Ž. Jovanović, M. Vukašinović-Sekulić, V. Mišković-Stanković, B. Obradović, *Carbohydr. Polym.*, **111**, 305 (2014).
47. Z. Jovanovic, A. Radosavljevic, J. Stojkovska, B. Nikolic, B. Obradovic, Z. Kacarevic-Popovic, V. Miskovic-Stankovic, *Polym. Compos.*, **35**, 217 (2014).
48. J. Liu, L. Cui, N. Kong, C. J. Barrow, W. Yang, *Eur. Polym. J.*, **50**, 9 (2014).
49. O. J. Botlhoko, S. S. Ray, J. Ramontja, *Eur. Polym. J.*, **102**, 130 (2018).
50. S. Shang, L. Gan, C. W. M. Yuen, S. X. Jiang, N. M. Luo, *Compos. Part A Appl. Sci. Manuf.*, **68**, 149 (2015).
51. J. Shen, M. Shi, N. Li, B. Yan, H. Ma, Y. Hu, M. Ye, *Nano Res.*, **3**, 339 (2010).
52. J. Ma, J. Zhang, Z. Xiong, Y. Yong, X. S. Zhao, *J. Mater. Chem.*, **21**, 3350 (2011).
53. Slistan-Grijalva, R. Herrera-Urbina, J. F. Rivas-Silva, M. Avalos-Borja, F. F. Castillon-Barraza, A. Posada-Amarillas, *Physica E*, **27**, 104 (2005).
54. X. Cai, M. Lin, S. Tan, W. Mai, Y. Zhang, Z. Liang, Z. Lin, X. Zhang, *Carbon*, **50**, 3407 (2012).
55. C. M. de Moraes, B. A. Lima, A. F. de Faria, M. Brocchi, O. L. Alves, *Int. J. Nanomedicine*, **10**, 6847 (2015).
56. M. Kozicki, M. Kołodziejczyk, M. Szynkowska, A. Pawlaczyk, E. Leśniewska, A. Matusiak, A. Adamus, A. Karolczak, *Carbohydr. Polym.*, **140**, 74 (2016).
57. S. H. Lim, S. M. Hudson, *J. Macromol. Sci. - Polym. Rev.*, **43**, 223 (2003).
58. C. M. Santos, M. C. R. Tria, R. A. M. V. Vergara, F. Ahmed, R. C. Advincula, D. F. Rodrigues, *Chem. Commun.*, **47**, 8892 (2011).
59. T. Taylor, C. Unakal, Staphylococcus Aureus. [Updated 2019 Mar 27]. *StatPearls [Internet]. Treasure Isl. StatPearls Publ. 2019 Jan-*. Available from https://www.ncbi.nlm.nih.gov/books/NBK441868 [Accessed 19.01.2020.], (2019).